

# Induction of Immunogenic Cell Death by Chemotherapeutic Platinum Complexes\*\*

Daniel Yuan Qiang Wong, Wendy Wei Fang Ong, and Wee Han Ang\*

**Abstract:** There is compelling evidence suggesting that the immune-modulating effects of many conventional chemotherapeutics, including platinum-based agents, play a crucial role in achieving clinical response. One way in which chemotherapeutics can engage a tumor-specific immune response is by triggering an immunogenic mode of tumor cell death (ICD), which then acts as an “anticancer vaccine”. In spite of being a mainstay of chemotherapy, there has not been a systematic attempt to screen both existing and upcoming Pt agents for their ICD ability. A library of chemotherapeutically active Pt agents was evaluated in an *in vitro* phagocytosis assay, and no correlation between cytotoxicity and phagocytosis was observed. A Pt<sup>II</sup> N-heterocyclic carbene complex was found to display the characteristic hallmarks of a type II ICD inducer, namely focused oxidative endoplasmic reticulum (ER) stress, calreticulin exposure, and both HMGB1 and ATP release, and thus identified as the first small-molecule immuno-chemotherapeutic agent.

Growing evidence suggests that conventional chemotherapeutics can modulate the immune system and trigger an immune response that sustains a long-term durable therapeutic outcome.<sup>[1]</sup> It has been proposed that the therapeutic efficacy of certain agents (e.g., anthracyclines, taxanes, and gemcitabine) depends, at least partially, on such off-target immune effects.<sup>[1a,2]</sup> Accordingly, higher densities of tumor-infiltrating lymphocytes following chemotherapy have been correlated with significantly better survival outcomes in colorectal and breast cancers.<sup>[3]</sup> One of several ways in which chemotherapeutics engage a tumor-specific immune response is by triggering immunogenic cell death (ICD), whereby the dying cancer cells initiate a robust immune response, acting as an “anticancer vaccine”.<sup>[4]</sup> Thus, immuno-competent (but not immunodeficient) mice vaccinated with dying cancer cells that had been pre-treated with ICD inducers (e.g., anthracyclines, shikonin, and hypericin–PDT)

are protected against subsequent challenges with live cancer cells.<sup>[5]</sup> Retrospective analysis of multiple cancers suggests that human patients treated with chemotherapy together with digoxin, an ICD-promoting agent, had an improved overall survival rate, especially when the chemotherapy cocktail did not already contain an ICD inducer.<sup>[6]</sup>

The ICD-inducing capacity of anticancer drugs has been tied with their capacity to elicit endoplasmic reticulum (ER) stress and the associated production of reactive oxygen species (ROS; Figure 1).<sup>[4,7]</sup> It is believed that cancer cells

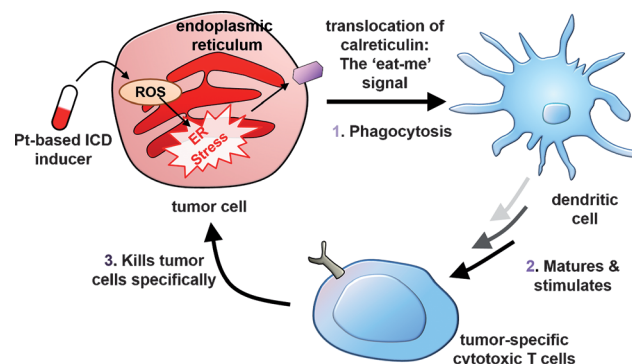


**Figure 1.** Schematic representation of drug-induced immunogenic cell death (ICD).

that dye in response to ROS-mediated ER stress emit a combination of three distinct spatiotemporally defined “danger” signals, which are recognized by the immune system and required for ICD.<sup>[6]</sup> These signals, which are now established as the biochemical hallmarks of ICD, are: 1) translocation of ER-resident calreticulin (CRT) to the cell surface during early apoptosis, 2) active secretion of ATP, and 3) extracellular secretion of nuclear high-mobility group box 1 protein (HMGB1) during late-stage apoptosis. Cell-surface CRT, the dominant pro-phagocytic “eat me” signal,<sup>[8]</sup> promotes the engulfment of cancer cells by professional macrophages, such as dendritic cells (DCs), for tumor antigen presentation.<sup>[5]</sup> Secreted ATP acts as a “find me” signal and stimulates purinergic P2RX7 receptors on DCs, triggering the production of IL-1 $\beta$ , a pro-inflammatory cytokine that is required for IFN- $\gamma$  production by tumor-specific cytotoxic T cells.<sup>[4,7]</sup> Finally, HMGB1 binds to toll-like receptor 4 (TLR4) on DCs, triggering a myeloid differentiation primary response gene 88 (MYD88) dependent signaling cascade, which promotes antigen processing and presentation to T cells.<sup>[4,7]</sup> Thus, a dysfunctional P2RX7 or TLR4 has been correlated with negative therapeutic outcomes in both mice

[\*] D. Y. Q. Wong,<sup>[†]</sup> W. W. F. Ong,<sup>[†]</sup> Prof. W. H. Ang  
Department of Chemistry, National University of Singapore  
3 Science Drive 3, Singapore (Singapore)  
E-mail: chmawh@nus.edu.sg

Prof. W. H. Ang  
NUS Graduate School of Integrative Sciences and Engineering  
28 Medical Drive, Singapore (Singapore)

[†] These authors contributed equally to this work.

[\*\*] We acknowledge the generous funding provided by the National University of Singapore and the Singapore Ministry of Education (R143-000-572-112 to A.W.H.).

Supporting information for this article is available on the WWW under <http://dx.doi.org/10.1002/anie.201500934>.

and human studies with ICD-inducing chemotherapeutics, such as doxorubicin, highlighting the immune component as an essential contribution to the efficacy of these agents.<sup>[4,7]</sup>

Although they have been a mainstay of chemotherapy, there has not been a systematic attempt to screen both existing and upcoming Pt agents for ICD. It has been reported that oxaliplatin, but not cisplatin, could induce ICD.<sup>[9]</sup> We evaluated a library of Pt-based compounds (Figure 2) that are

nor ER ROS (Supporting Information, Figure S1).<sup>[9]</sup> Nonetheless, there was a certain concentration dependence observed with cisplatin (50 and 100  $\mu\text{M}$ ) and Pt-NHC (1 and 5  $\mu\text{M}$ ), which correlated well with qualitative measurements of ER ROS (Figure S1). The addition of 2 axial acetato ligands to JM118 elevated phagocytosis in satraplatin, which could reflect differences in subcellular localization or accumulation. Phagocytosis was corroborated by fluorescence microscopy,

which showed cytosolic mixing of the green and red dyes at the area of contact between CT-26 and J774 cells (Figure 3a).

We determined that the observed phagocytosis was indeed mediated by cell-surface exposure of CRT. Although other recognition ligands have been identified,<sup>[15]</sup> ecto-CRT was shown to be the dominant eat-me signal and key mediator of immunogenicity in cancer cells.<sup>[8,16]</sup> CRT, normally located in the ER, would be translocated to the outer surface of the plasma membrane in response to ER stress.<sup>[4b]</sup>

This would then be recognized by low-density lipoprotein-related protein (LRP) receptors on the macrophages. Coating the cell surface with recombinant murine CRT to CT-26 without drug or with 50  $\mu\text{M}$  cisplatin resulted in a significant increase in tumor-cell phagocytosis over basal levels (Figure 3c). On the other hand, blocking the CRT–LRP interactions with a CRT blocking peptide abolished phagocytosis of Pt-NHC-treated CT-26 (Figure 3c). Hence, these results underscored the requirement of ecto-CRT on tumor cells for inducing phagocytosis in our screening method.

We proceeded to evaluate the capacity of Pt-NHC to elicit the distinct biochemical hallmarks of ICD, namely CRT exposure, ATP secretion, and extracellular HMGB1 release. Surface immunostaining under non cell-permeabilizing conditions indicated that CRT exposure with Pt-NHC (5  $\mu\text{M}$ ) was a rapid process, detectable as quickly as one hour after drug-exposure (Figure 3d,e). Furthermore, surface CRT was detected on treated cells with intact membrane integrity and also before exposure to phosphatidylserine, implying that the translocation occurred at an early stage of apoptosis (Figure 3e). Under identical conditions, no immuno-detectable CRT was observed on the surface of non-treated cells. Confocal microscopy analysis of cells treated with either Pt-NHC (5  $\mu\text{M}$ ) or cisplatin (100  $\mu\text{M}$ ) revealed that ecto-CRT was distributed in uneven clusters, which was consistent with prior studies on other ICD inducers (Figure 3d).<sup>[9,16–17]</sup> It was proposed that the uneven distribution reflected the segregation of CRT away from CD47 (the “don’t-eat-me” signal) and thus promoted phagocytosis.<sup>[16]</sup> The release of both ATP and HMGB1 was also clearly evident with Pt-NHC treatment

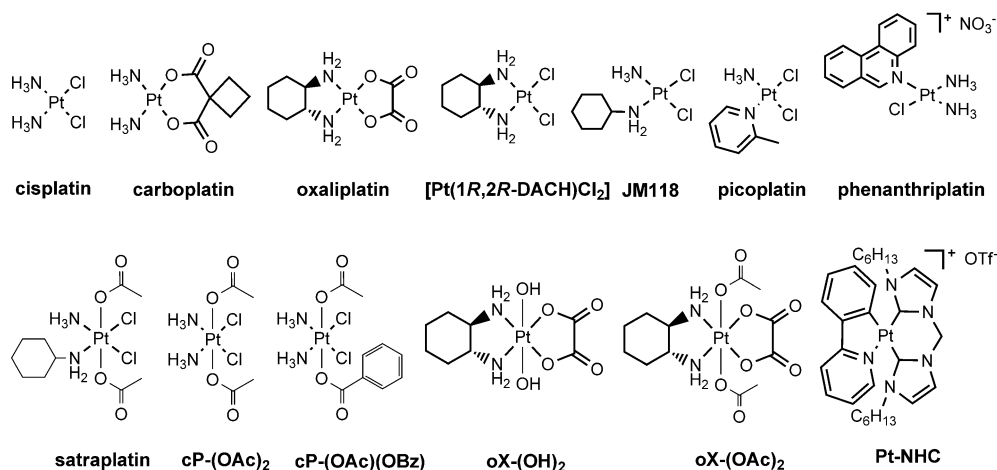
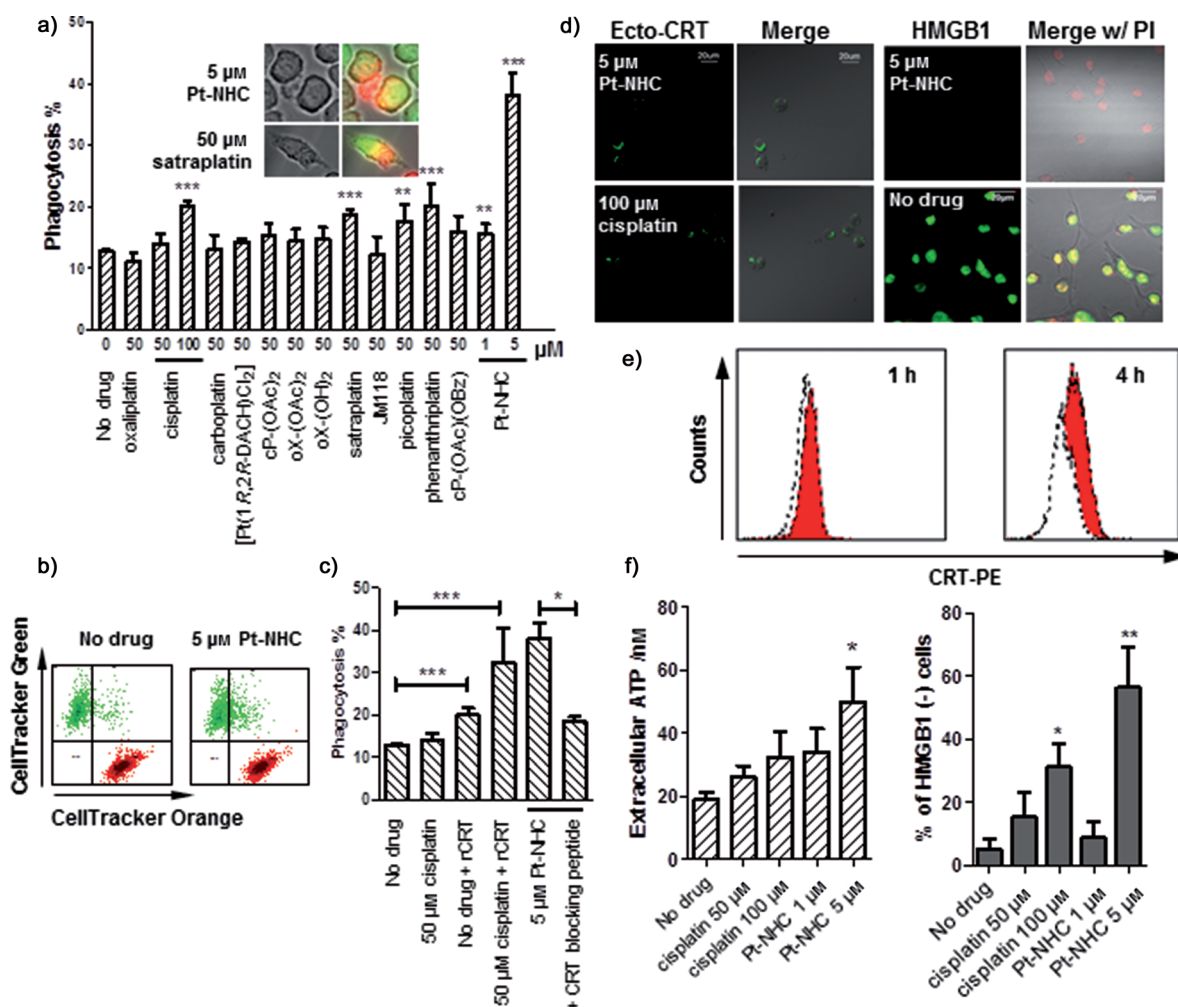


Figure 2. Structures of Pt agents used in this study.

either clinically relevant or of upcoming interest as well as structurally related analogues. The library includes cisplatin, oxaliplatin, and carboplatin, all of which are in clinical use.<sup>[11]</sup> [Pt(1R,2R-DACH)Cl<sub>2</sub>] is a structural analogue of oxaliplatin. Picoplatin, satraplatin, and phenanthriplatin are examples of novel Pt compounds either in clinical trials or pre-clinical development whereas JM118 is the active Pt<sup>II</sup> species of satraplatin.<sup>[12]</sup> Pt-NHC is a unique cyclometalated complex that selectively localizes in the ER and induces ER stress.<sup>[13]</sup> The remaining complexes are Pt<sup>IV</sup> prodrugs of cisplatin and oxaliplatin.

As a critical step for ICD is the engulfment of dying cancer cells by professional macrophages,<sup>[5]</sup> we first applied an in vitro phagocytosis assay<sup>[14]</sup> to identify possible ICD inducers. Briefly, murine CT-26 tumor cells (pre-stained with CellTracker Orange) were treated (4 h) before co-incubation (2 h) with murine J774 macrophages (pre-stained with CellTracker Green). Double-stained macrophages indicated phagocytosis (Figure 3b). With the exception of Pt-NHC, which was both very cytotoxic and fluorescent at concentrations above 10  $\mu\text{M}$ , all other Pt agents were screened at 50  $\mu\text{M}$ . Pt-NHC (5  $\mu\text{M}$ ) sharply increased tumor-cell phagocytosis compared with non-treated controls ( $38.2 \pm 3.5\%$  vs.  $12.8 \pm 0.2\%$ ,  $p < 0.0001$ ) followed distantly by phenanthriplatin ( $20.1 \pm 3.6\%$ ), cisplatin ( $20.0 \pm 1.0\%$  at 100  $\mu\text{M}$  only), satraplatin ( $18.8 \pm 0.9\%$ ), and picoplatin ( $17.6 \pm 2.8\%$ ; Figure 3a). In contrast, none of the clinically used Pt drugs nor their related analogues promoted phagocytosis at 50  $\mu\text{M}$ . Our results diverged from a recent study where oxaliplatin could induce ICD as we observed neither increased phagocytosis



**Figure 3.** Phagocytosis screening. a) Orange-stained CT-26 cells were drug-treated (4 h) before co-incubating (2 h) with green-stained J774 macrophages and analyzed by flow cytometry. The percentage of phagocytosis was calculated from the number of double-stained macrophages over the total number of macrophages. Inset: Fluorescence microscopy of J774 macrophages (green) engulfing CT-26 (red) as evident by mixing of the dyes. b) Representative flow cytometry scatter plots showing increased phagocytosis (top right quadrant) with Pt-NHC over control. c) Coating CT-26 with rCRT enabled phagocytosis whereas co-incubation with a CRT blocking peptide abolished phagocytosis. Mean  $\pm$  SEM (\*  $p < 0.05$ , \*\*  $p < 0.01$ , \*\*\*  $p < 0.0001$ ; Student's *t* test; SEM = standard error of the mean). ICD indicators: d) Left: Rapid patch-like surface exposure of CRT observed by confocal microscopy after drug treatment (1 h) of CT-26 followed by surface immuno-fluorescence staining with anti-CRT mAb. Right: HMGB1 release from the nuclei of CT-26 after 24 h drug exposure (permeabilized and stained with both anti-HMGB1-Dy488 mAb and PI). e) Pt-NHC enhanced ecto-CRT exposure in live cells (red-shaded) compared to non-treated control (dotted line). CT26 cells were treated for one hour (gated against PI cells) and four hours (gated against Annexin V cells) and surface-stained with an anti-CRT-PE mAb. f) Extracellular release of ATP (left) and HMGB1 (right) of CT-26 after exposure for 24 hours. Mean  $\pm$  SEM (\*  $p < 0.05$ , \*\*  $p < 0.01$ ; Student's *t* test).

(5  $\mu$ M). ATP secretion into the supernatant 24 hours after the treatment was measured in a luciferase-based assay (Figure 3f). The extracellular release of nuclear HMGB1 was detected as an absence of nuclear fluorescence after staining (with Triton-X permeabilization) of treated cells (24 h) with an anti-HMGB1-Dy488 antibody and subsequent analysis by both confocal microscopy (Figure 3d) and flow cytometry (Figure 3f). In contrast, the presence of nuclear HMGB1 was clearly evident in non-drug-treated controls. Thus, Pt-NHC fulfilled all three molecular hallmarks of ICD, a feature unique to all other validated ICD inducers, such as UVC irradiation, anthracyclines, and cardiac glycosides.<sup>[4,6]</sup>

It is believed that ER stress, either in tandem with or in parallel to an over-generation of ROS, plays a prominent role

in ICD. The ER stress response elicited by ICD inducers would ignite a cascade of danger signaling pathways, including the activation of protein-kinase-like ER kinase (PERK), which is mandatory for CRT exposure and possibly ATP secretion.<sup>[4,7,18]</sup> Nonetheless, not all ER stressors (e.g., tunicamycin) are ICD inducers but the converse was a prerequisite.<sup>[7]</sup> ICD inducers have been classified into two categories: Type I inducers trigger ER stress through off-target secondary mechanisms whereas type II inducers selectively trigger focused ROS-mediated ER stress and were shown to be more efficient in emitting danger signals.<sup>[4b,17,19]</sup> Type II ICD inducers are believed to be superior to the more common type I inducers, which only induce collateral ER stress.<sup>[4b,10]</sup> To date, only a handful of type II ICD inducers



have been identified (e.g., photodynamic therapy with hypericin, an ER-specific photosensitizer, and certain oncolytic viruses).<sup>[4b]</sup> Pt-NHC, which has a minimal DNA binding affinity, was previously reported to specifically localize in the ER and induce an ER stress response through PERK activation.<sup>[13]</sup>

In this context, we sought to demonstrate that the ER stress response was in fact ROS-mediated, qualifying Pt-NHC as a Type II ICD inducer. ROS production was tracked after short-term drug exposure (4 h) using 2',7'-dichlorodihydrofluorescein diacetate (H<sub>2</sub>DCFDA) as a general ROS indicator,<sup>[20]</sup> and the ER was visualized with ER Tracker Red, which bind to the sulfonyleurea receptors on ER. In MDA-MB-231, there was a clear colocalization of ROS with the ER (89.2 % as determined by the Costes method)<sup>[21]</sup> with Pt-NHC (1  $\mu$ M; Figure S1). At 5  $\mu$ M Pt-NHC, the ER exhibited severe deformation, and ROS were correspondingly more diffuse and less colocalized, possibly as a consequence of increased ER membrane permeability associated with ER-stress-induced apoptosis.<sup>[22]</sup> In CT-26, ROS was only observed with 5  $\mu$ M Pt-NHC, but not at 1  $\mu$ M. In keeping with MDA-MB-231, the observed ROS were relatively diffuse. The absence of ROS with Pt-NHC at a lower concentration (1  $\mu$ M) corresponded to significantly lower phagocytosis, ATP secretion, and HMGB1 release, implying that the ROS played a key role in Pt-NHC associated ICD. Likewise, phagocytosis was only observed with cisplatin at 100  $\mu$ M (where intense formation of ROS was observed in a subpopulation of cells), but not at 50  $\mu$ M (a concentration where ROS were not observed). In general, all Pt compounds that promoted phagocytosis had measurable ROS production (Figure S1). Phagocytosis induced by Pt-NHC was significantly reduced when tumor cells were co-incubated with trolox, an antioxidant that quenches ROS (Figure 4). Thus, oxidative ER stress triggered by Pt-NHC plays a crucial role in ICD.

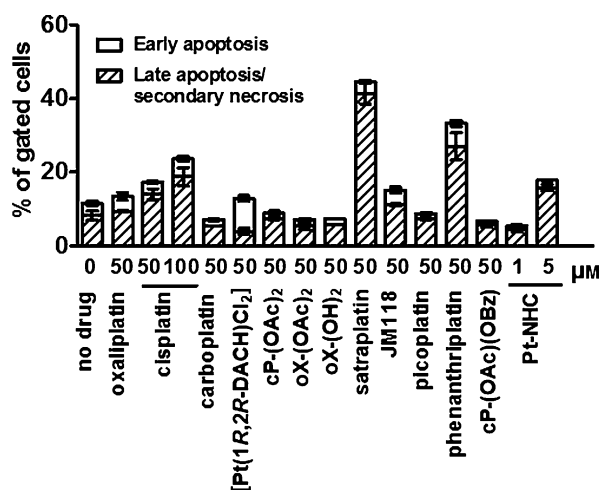


**Figure 4.** The anti-oxidant trolox quenches cellular ROS, which in turn inhibits phagocytosis. CT-26 was pre-treated with trolox (30 min) prior to drug exposure and later co-treated with trolox and Pt-NHC (4 h). a) Trolox quenched Pt-NHC induced ROS as analyzed by flow cytometry. b) Co-incubation of Pt-NHC with trolox significantly inhibited tumor-cell phagocytosis. Mean  $\pm$  SEM (\*  $p < 0.05$ , \*\*  $p < 0.01$ ; Student's  $t$  test).

Traditionally, new platinum agents have been evaluated primarily by studying their direct cytotoxicity against cancer cell lines. We observed no correlation between the propensity of Pt agents to trigger tumor-cell phagocytosis and cytotoxicity (Figure 5, evaluated in an Annexin V assay), suggesting

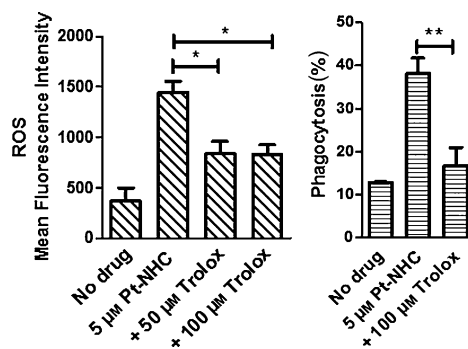


**Figure 5.** Cytotoxicity of Pt agents in an Annexin V apoptosis assay. CT-26 cells were treated for 24 hours and stained with Annexin V/eGFP and propidium iodide. Mean  $\pm$  SEM.

that ICD is independent of cytotoxicity. It was demonstrated that the therapeutic efficacy of anthracyclines (an ICD inducer) was negated in mice models when the host immune system was compromised.<sup>[2,23]</sup> This observation suggests that, at least in some models of cancer, it was the immune-modulating capacity of the chemotherapeutics and not the cytotoxicity that was important. In keeping with this strategy, we recently reported platinum(IV)–peptide agents that directly activated macrophages as another pathway of eliciting an anticancer immune response.<sup>[24]</sup>

Over the last decade, there has been substantial evidence supporting the pivotal role of the immune system in inducing tumor regression following conventional chemotherapy.<sup>[1]</sup> It is probable that many highly promising immunogenic and/or immune-stimulating Pt candidates might have been neglected. This work, which represents one of the very first attempts to exploit the immune-modulating properties of Pt agents, could pave the way for the development of combined Pt-based immuno-chemotherapeutics.

**Keywords:** antitumor agents · immuno-chemotherapy · immunogenic cell death · oxidative stress · platinum

**How to cite:** *Angew. Chem. Int. Ed.* **2015**, *54*, 6483–6487  
*Angew. Chem.* **2015**, *127*, 6583–6587

- [1] a) L. Galluzzi, L. Senovilla, L. Zitvogel, G. Kroemer, *Nat. Rev. Drug Discovery* **2012**, *11*, 215–233; b) L. Zitvogel, L. Galluzzi, M. J. Smyth, G. Kroemer, *Immunity* **2013**, *39*, 74–88.
- [2] S. R. Mattarollo, S. Loi, H. Duret, Y. Ma, L. Zitvogel, M. J. Smyth, *Cancer Res.* **2011**, *71*, 4809–4820.
- [3] a) N. Halama, S. Michel, M. Kloor, I. Zoernig, A. Benner, A. Spille, T. Pommerenke, D. M. von Knebel, G. Folprecht, B. Lubber, N. Feyen, U. M. Martens, P. Beckhove, S. Gnjatic, P. Schirmacher, E. Herpel, J. Weitz, N. Grabe, D. Jaeger, *Cancer Res.* **2011**, *71*, 5670–5677; b) M. V. Dieci, C. Criscitiello, A. Goubar, G. Viale, P. Conte, V. Guarneri, G. Ficarra, M. C.

- Mathieu, S. Delaloge, G. Curigliano, F. Andre, *Ann. Oncol.* **2014**, *25*, 611–618.
- [4] a) G. Kroemer, L. Galluzzi, O. Kepp, L. Zitvogel, *Annu. Rev. Immunol.* **2013**, *31*, 51–72; b) D. V. Krysko, A. D. Garg, A. Kaczmarek, O. Krysko, P. Agostinis, P. Vandenabeele, *Nat. Rev. Cancer* **2012**, *12*, 860–875.
- [5] M. Obeid, A. Tesniere, F. Ghiringhelli, G. M. Fimia, L. Apetoh, J. L. Perfettini, M. Castedo, G. Mignot, T. Panaretakis, N. Casares, D. Métié, N. Larochette, P. van Endert, F. Ciccosanti, M. Piacentini, L. Zitvogel, G. Kroemer, *Nat. Med.* **2007**, *13*, 54–61.
- [6] L. Menger, E. Vacchelli, S. Adjemian, I. Martins, Y. Ma, S. Shen, T. Yamazaki, A. Q. Sukkurwala, M. Michaud, G. Mignot, F. Schlemmer, E. Sulpice, C. Locher, X. Gidrol, F. Ghiringhelli, N. Modjtahedi, L. Galluzzi, F. André, L. Zitvogel, O. Kepp, G. Kroemer, *Sci. Transl. Med.* **2012**, *4*, 143ra99.
- [7] O. Kepp, L. Menger, E. Vacchelli, C. Locher, S. Adjemian, T. Yamazaki, I. Martins, A. Q. Sukkurwala, M. Michaud, L. Senovilla, L. Galluzzi, G. Kroemer, L. Zitvogel, *Cytokine Growth Factor Rev.* **2013**, *24*, 311–318.
- [8] M. P. Chao, S. Jaiswal, R. Weissman-Tsukamoto, A. A. Alizadeh, A. J. Gentles, J. Volkmer, K. Weiskopf, S. B. Willingham, T. Raveh, C. Y. Park, R. Majeti, I. L. Weissman, *Sci. Transl. Med.* **2010**, *2*, 63ra94.
- [9] A. Tesniere, F. Schlemmer, V. Boige, O. Kepp, I. Martins, F. Ghiringhelli, L. Aymeric, M. Michaud, L. Apetoh, L. Barault, J. Mendiboure, J. P. Pignon, V. Jooste, P. van Endert, M. Ducreux, L. Zitvogel, F. Piard, G. Kroemer, *Oncogene* **2010**, *29*, 482–491.
- [10] H. Inoue, K. Tani, *Cell Death Differ.* **2014**, *21*, 39–49.
- [11] N. Shah, D. S. Dizon, *Future Oncol.* **2009**, *5*, 33–42.
- [12] a) G. Y. Park, J. J. Wilson, Y. Song, S. J. Lippard, *Proc. Natl. Acad. Sci. USA* **2012**, *109*, 11987–11992; b) A. Bhargava, U. N. Vaishampayan, *Expert Opin. Investig. Drugs* **2009**, *18*, 1787–1797; c) J. Holford, S. Y. Sharp, B. A. Murrer, M. Abrams, L. R. Kelland, *Br. J. Cancer* **1998**, *77*, 366–373.
- [13] T. Zou, C. N. Lok, Y. M. Fung, C. M. Che, *Chem. Commun.* **2013**, *49*, 5423–5425.
- [14] P. R. Hoffmann, A. M. deCathelineau, C. A. Ogden, Y. Leverrier, D. L. Bratton, D. L. Daleke, A. J. Ridley, V. A. Fadok, P. M. Henson, *J. Cell Biol.* **2001**, *155*, 649–659.
- [15] J. Savill, I. Dransfield, C. Gregory, C. Haslett, *Nat. Rev. Immunol.* **2002**, *2*, 965–975.
- [16] S. J. Gardai, K. A. McPhillips, S. C. Frasch, W. J. Janssen, A. Starefeldt, J. E. Murphy-Ullrich, D. L. Bratton, P.-A. Oldenborg, M. Michalak, P. M. Henson, *Cell* **2005**, *123*, 321–334.
- [17] A. D. Garg, D. V. Krysko, P. Vandenabeele, P. Agostinis, *Cancer Immunol. Immunother.* **2012**, *61*, 215–221.
- [18] A. D. Garg, D. V. Krysko, T. Verfaillie, A. Kaczmarek, G. B. Ferreira, T. Marysael, N. Rubio, M. Firczuk, C. Mathieu, A. J. M. Roebroek, W. Annaert, J. Golab, P. de Witte, P. Vandenabeele, P. Agostinis, *EMBO J.* **2012**, *31*, 1062–1079.
- [19] A. D. Garg, D. V. Krysko, P. Vandenabeele, P. Agostinis, *OncolImmunology* **2012**, *1*, 786–788.
- [20] S. L. Hempel, G. R. Buettner, Y. Q. O'Malley, D. A. Wessels, D. M. Flaherty, *Free Radic. Biol. Med.* **1999**, *27*, 146–159.
- [21] S. V. Costes, D. Daelemans, E. H. Cho, Z. Dobbin, G. Pavlakis, S. Lockett, *Biophys. J.* **2004**, *86*, 3993–4003.
- [22] X. Wang, K. E. Olberding, C. White, C. Li, *Cell Death Differ.* **2011**, *18*, 38–47.
- [23] A. Q. Sukkurwala, S. Adjemian, L. Senovilla, M. Michaud, S. Spaggiari, E. Vacchelli, E. E. Baracco, L. Galluzzi, L. Zitvogel, O. Kepp, G. Kroemer, *OncolImmunology* **2014**, *3*, e28473.
- [24] D. Y. Q. Wong, C. H. F. Yeo, W. H. Ang, *Angew. Chem. Int. Ed.* **2014**, *53*, 6752–6756; *Angew. Chem.* **2014**, *126*, 6870–6874.

Received: February 1, 2015

Published online: April 14, 2015